



1 **A large role of missing volatile organic compounds reactivity**
2 **from anthropogenic emissions in ozone pollution regulation**

3 Wenjie Wang^{1,2*}, Bin Yuan^{1*}, Hang Su², Yafang Cheng², Jipeng Qi¹, Sihang Wang¹,
4 Wei Song³, Xinming Wang³, Chaoyang Xue², Chaoqun Ma², Fengxia Bao², Hongli
5 Wang⁴, Shengrong Lou⁴, Min Shao¹

6 ¹ Institute for Environmental and Climate Research, Jinan University,
7 Guangzhou 511443, China

8 ² Multiphase Chemistry Department, Max Planck Institute for Chemistry, Mainz
9 55128, Germany

10 ³ State Key Laboratory of Organic Geochemistry, Guangzhou Institute of
11 Geochemistry, Chinese Academy of Sciences, Guangzhou 510640, China

12 ⁴ State Environmental Protection Key Laboratory of Formation and Prevention of
13 Urban Air Pollution Complex, Shanghai Academy of Environmental Sciences,
14 Shanghai 200233, China

15

16

17 **Correspondence to:* Bin Yuan (byuan@jnu.edu.cn);
18 Wenjie Wang (Wenjie.Wang@mpic.de)

19



20 **Abstract:** There are thousands of VOC species in ambient air, while existing techniques
21 can only detect a small part of them (~ several hundred). The large number of
22 unmeasured VOCs prevents us from understanding the photochemistry of ozone and
23 aerosols in the atmosphere. The major sources and photochemical effects of these
24 unmeasured VOCs in urban areas remain unclear. The missing VOC reactivity, which
25 is defined as the total OH reactivity of the unmeasured VOCs, is a good indicator to
26 constrain the photochemical effect of unmeasured VOCs. Here, we identified the
27 dominant role of anthropogenic emission sources in the missing VOC reactivity
28 (accounting for up to 70%) by measuring missing VOC reactivity and tracer-based
29 source analysis in a typical megacity in China. Omitting the missing VOC reactivity
30 from anthropogenic emissions in model simulations will remarkably affect the
31 diagnosis of sensitivity regimes for ozone formation, overestimating the degree of
32 VOC-limited regime by up to 46%. Therefore, a thorough quantification of missing
33 VOC reactivity from various anthropogenic emission sources is urgently needed for
34 constraints of air quality models and the development of effective ozone control
35 strategies.

36

37



38 1 Introduction

39 Volatile organic compounds (VOCs) are key precursors of major photochemical
40 pollutants, including ozone (O₃) and secondary organic aerosols (Atkinson,
41 2000; Atkinson and Arey, 2003). Severe O₃ and particle pollution are frequently related
42 to high emissions of VOCs (Atkinson and Arey, 2003; Monks et al., 2015). There exist
43 thousands of VOC species in ambient air that are emitted from either natural processes
44 or anthropogenic activities (Goldstein and Galbally, 2007). No one instrument can
45 capture all VOCs out there and even when they can be measured there is information
46 missing on identification and properties (Yuan et al., 2017; Wang et al., 2014). As a
47 result, the total amount of VOCs in ambient air has generally been underestimated. By
48 now, emission inventories of VOCs used in air quality models only include the VOC
49 species that can be measured, which will lead to an underestimation of the
50 photochemical effect of total VOCs and thus causes uncertainties in predicting
51 secondary pollution. The quantification of the unmeasured VOCs is crucial to assess
52 secondary pollution precisely.

53 The measurement of total OH reactivity (R_{OH}) provides an effective approach to
54 quantify the total amount of reactive gases in terms of reacting with OH radicals. The
55 total OH reactivity is defined as:

$$56 R_{OH} = \sum_i k_{OH+X_i} [X_i], \quad (1)$$

57 where X represents a reactive species including carbon monoxide (CO), nitrogen
58 oxides (NO_x) and VOCs etc., and k_{OH+X_i} is the reaction rate constant for the oxidation
59 of species X by OH. The measured R_{OH} is higher than that calculated based solely on
60 the measured reactive species, and the difference between them is mostly from
61 unmeasured VOCs (Yang et al., 2017). Missing VOC reactivity (missing VOC_R),
62 defined as VOC reactivity (VOC_R) of all unmeasured VOCs, can be obtained by
63 subtracting the calculated R_{OH} from the measured R_{OH}.

$$64 \text{missing VOC}_R = \text{measured } R_{OH} - \text{calculated } R_{OH} \quad (2)$$

$$65 \text{calculated } R_{OH} = \sum_i k_{OH+\text{reactive species}_i} [\text{reactive species}_i] \quad (3)$$



66 where reactive species represents measured VOCs and reactive inorganic species
67 including carbon monoxide (CO), nitric oxide (NO), nitrogen dioxide (NO₂), O₃, sulfur
68 dioxide (SO₂) and so on. The missing VOC_R provides a constraint for evaluating the
69 photochemical roles of unmeasured VOCs in the atmosphere (Sadanaga et al.,
70 2005; Yang et al., 2016b). The inclusion of the missing VOC_R can help to improve the
71 model performance in simulating photochemistry processes. Relatively high missing
72 VOC_R have been found in forests (Di Carlo et al., 2004; Hansen et al., 2014; Nakashima
73 et al., 2014; Nölscher et al., 2016; Praplan et al., 2019), urban areas (Shirley et al.,
74 2006; Yoshino et al., 2006; Dolgorouky et al., 2012; Yang et al., 2017) and suburban areas
75 (Kovacs et al., 2003; Yang et al., 2017; Fuchs et al., 2017; Lou et al., 2010), accounting
76 for 10-75% of total ROH.

77 The potential sources of missing VOC_R include anthropogenic emissions, biogenic
78 emissions, soil emissions, and photochemical production, etc. (Yang et al., 2016b).
79 Previous studies have reported that the missing VOC_R in forest areas was mainly from
80 either direct emissions or photochemical oxidation of biogenic VOCs (Di Carlo et al.,
81 2004; Hansen et al., 2014; Nakashima et al., 2014; Nölscher et al., 2016; Praplan et al.,
82 2019). Nevertheless, the dominant source of the missing VOC_R in urban and suburban
83 areas remains unclear or under debate.

84 Surface O₃ pollution has become a major public health concern in cities worldwide
85 (Paoletti et al., 2014; Lefohn et al., 2018). A critical issue in determining an emission
86 control strategy for ozone pollution is to understand the relative benefits of NO_x and
87 VOC emission controls. This is generally framed in terms of ozone precursor sensitivity,
88 i.e., whether ozone production is NO_x-limited or VOC-limited (Kleinman,
89 1994; Sillman et al., 1990). Nevertheless, the effect of missing VOCs on ozone
90 precursor sensitivity has not been well understood yet. Given that the missing VOC_R
91 accounts for a large part of total VOC_R, clearly clarifying the role of missing VOC_R in
92 determining ozone precursor sensitivity is an urgent need for the diagnosis of ozone
93 sensitivity regimes and formulation of an effective emission reduction roadmap.

94 China has become a global hot spot of ground-level ozone pollution in recent years



95 (Lu et al., 2018; Wang et al., 2022). Pearl River Delta (PRD) remains one of the most
96 O₃-polluted regions in China (Li et al., 2022), although many control measures have
97 been attempted. Here, we measured R_{OH} in Guangzhou, a megacity in PRD and
98 quantified the missing VOC_R. The dominant source of the missing VOC_R and its impact
99 on ozone precursor sensitivity were comprehensively investigated.

100 **2 Method**

101 **2.1 R_{OH} measurement**

102 The field campaign was conducted from 25 September to 30 October 2018 at an
103 urban site in downtown Guangzhou (113.2°E, 23°N). This site is primarily influenced
104 by industrial and vehicular emissions.

105 Total R_{OH} was measured by the comparative reactivity method (CRM) (Sinha et
106 al., 2008). The CRM system consists of three major components, namely an inlet and
107 calibration system, a reactor, and a measuring system. Here, pyrrole (C₄H₅N) was used
108 as the reference substance in CRM and its concentration was quantified by a quadrupole
109 proton-transfer-reaction mass spectrometer (PTR-MS) (Ionicon Analytik GmbH,
110 Innsbruck, Austria). The CRM system was calibrated by propane, propene, toluene
111 standards and 16 VOC mixed standard (acetaldehyde, methanol, ethanol, isoprene,
112 acetone, acetonitrile, methyl vinyl ketone, methyl ethyl ketone, benzene, toluene, o-
113 xylene, α -pinene, 1,2,4-trimethylbenzene, phenol, m-cresol and naphthalene).
114 Measured and calculated R_{OH} agreed well within 15% for all calibrations. The R_{OH}
115 measurement by the CRM method is interfered from ambient nitric oxide (NO), which
116 produces additional OH radicals via the reaction of HO₂ radicals with NO (Sinha et al.,
117 2008). To correct this interference, a series of experiments were conducted by
118 introducing different levels of NO (0–100 ppb) and given amounts of VOC into the
119 CRM reactor. A correction curve was acquired from these NO interference experiments,
120 which can be used to correct the R_{OH} thank to the simultaneous measurement of ambient
121 NO concentrations. The detection limits of the CRM method were around 2.5 s⁻¹, and



122 the total uncertainty was estimated to be about 15%. The CRM method has been
123 successfully applied to measure OH reactivity in urban areas with high NO_x levels in
124 previous studies (Dolgorouky et al., 2012; Yang et al., 2017; Hansen et al., 2015). The
125 intercomparison between the CRM method and pump–probe technique indicates that
126 the CRM method can be used under high-NO_x conditions (NO_x>10 ppb) if a NO_x -
127 dependent correction is carefully applied (Hansen et al., 2015).

128 **2.2 VOCs measurements**

129 Nonmethane hydrocarbons (NMHCs) were measured using a gas chromatograph–
130 mass spectrometer/flame ionization detector (GC–MS/FID) system coupled with a
131 cryogen-free preconcentration device (Wang et al., 2014). The system contains two-
132 channel sampling and GC column separation, which is able to measure C₂–C₅
133 hydrocarbons with the FID in one channel and measure C₅–C₁₂ hydrocarbons using
134 MS detector in the other channel. A total of 56 NMHCs species were measured. The
135 time resolution of the measurement was 1 h. The uncertainties of VOC measurements
136 by GC–MS/FID are in the range of 15 %–20 % (Wang et al., 2014; Yuan et al., 2012).

137 An online proton-transfer-reaction time-of-flight mass spectrometer (PTR-ToF-
138 MS) (Ionicon Analytic GmbH, Innsbruck, Austria) with H₃O⁺ and NO⁺ ion sources was
139 also used to measure VOCs. PTR-ToF-MS technique is capable of measuring
140 oxygenated VOCs (OVOCs) and higher alkanes that GC–MS/FID can not measure
141 (Wang et al., 2020a; Wu et al., 2020). The time resolution of PTR-ToF-MS
142 measurements was 10 s. A total of 31 VOCs were calibrated using either gas or liquid
143 standards. For other measured VOCs, we used the method proposed by Sekimoto et al.
144 (2017) to determine the relationship between VOC sensitivity and kinetic rate constants
145 for proton transfer reactions of H₃O⁺ with VOCs. The fitted line was used to determine
146 the concentrations of those uncalibrated species. The uncertainties of the concentrations
147 for uncalibrated species were about 50 % (Sekimoto et al., 2017). The PTR-ToF-MS is
148 capable of measuring additional VOC species that GC–MS/FID cannot measure
149 including NMHCs with more carbons (C₁₂–C₂₀) and OVOCs including aldehydes,



150 ketones, carboxylic acids, alcohols and nitrophenols. Formaldehyde (HCHO) was
151 measured by a custom-built instrument based on the Hantzsch reaction and absorption
152 photometry (Xu et al., 2022).

153 **2.3 Other measurements**

154 Nitrous acid (HONO) was measured by a custom-built LOPAP (Long Path
155 Absorption Photometer) based on wet chemical sampling and photometric detection
156 (Yu et al., 2022). The uncertainty of the measurement was 8 %. NO_x, O₃, sulfur dioxide
157 (SO₂) and CO were measured by NO_x analyzer (Thermo Scientific, Model 42i), O₃
158 analyzer (Thermo Scientific, Model 49i), SO₂ analyzer (Thermo Scientific, Model 43i)
159 and CO analyzer (Thermo Scientific, Model 48i), respectively. The meteorological data,
160 including temperature (T), relative humidity (RH) and wind speed and direction (WS,
161 WD) were recorded by Vantage Pro2 Weather Station (Davis Instruments Inc., Vantage
162 Pro2) with a time resolution of 1 min. Photolysis frequencies of O₃, NO₂, HONO, H₂O₂,
163 HCHO and NO₃ were measured by a spectrometer (Focused Photonics Inc., PFS-100)
164 (Shetter and Müller, 1999; Wang et al., 2019).

165 **2.4 Multiple linear regression**

166 The multiple linear regression (MLR) have been successfully applied to quantify
167 the sources of air pollutants (Li et al., 2019; Yang et al., 2016a). In this study, a tracer-
168 based MLR analysis was used to decouple the individual contributions of
169 anthropogenic emissions, secondary production, biogenic emissions and background
170 level to missing VOC_R, as shown in Eq. (4).

$$171 \quad \text{Missing VOC}_R = a[\text{CO}] + b[\text{O}_x] + c[\text{isoprene}_{\text{initial}}] + C_{\text{background}} \quad (4)$$

172 where O_x is defined as O₃+NO₂. [CO], [O_x] and [isoprene_{initial}] are concentrations
173 of tracers for anthropogenic emissions, secondary production and biogenic emissions,
174 respectively. [isoprene_{initial}] represents the initial concentration of isoprene from
175 biogenic emissions that has not undergone any photochemical reactions, which is
176 calculated from observed isoprene and its photochemical products MVK and MACR



177 (Xie et al., 2008). $C_{background}$ indicates the background level of missing VOC_R. a, b,
178 c and $C_{background}$ are fitted coefficients by the multiple linear regression.

179 2.5 Observation-based box model

180 A zero-dimensional box model coupled with the Master Chemical Mechanism
181 (MCM) v3.3.1 chemical mechanism (Jenkin et al., 2003) was used to simulate the
182 photochemical production of RO_x (RO_x=OH+HO₂+RO₂) radicals and O₃ during the
183 field campaign. The model was constrained by the observations of meteorological
184 parameters, photolysis frequencies, VOCs, NO, NO₂, O₃, CO, SO₂ and HONO. The
185 model runs were performed in a time-dependent mode with a time resolution of 1 hour
186 and a spin-up of four days. A 24-h lifetime was introduced for all simulated species,
187 including secondary species and radicals, to approximately simulate dry deposition and
188 other losses of these species (Lu et al., 2013; Wang et al., 2020b). Sensitivity tests show
189 that this assumed physical loss lifetime has a relatively small influence on RO_x radicals
190 and ozone production rates.

191 Measured OVOCs such as HCHO, acetaldehyde and acetone were constrained in
192 the model and unmeasured OVOCs were simulated according to the photochemical
193 oxidation of NMHCs by OH radicals. RO₂, HO₂ and OH radicals were simulated by the
194 box model to calculate the net O₃ production rate (P(O₃)) and O₃ loss rate (L(O₃)) as
195 shown in Equations (5) and (6) as derived by Mihelcic et al. (2003)

$$196 \quad P(O_3) = k_{HO_2+NO}[HO_2][NO] + \sum_i(k_{RO_2+NO}^i[RO_2^i][NO]) - k_{OH+NO_2}[OH][NO_2] - L(O_3)$$

197

$$(5)$$

$$198 \quad L(O_3) = (\theta j(O^1D) + k_{OH+O_3}[OH] + k_{HO_2+O_3}[HO_2] + \sum_j(k_{alkene+O_3}^j[alkene^j])[O_3]$$

199

$$(6)$$

200 where θ is the fraction of O¹D from ozone photolysis that reacts with water vapor, and
201 i and j represent the number of species of RO₂ and alkenes, respectively.



202 **3 Results and discussion**

203 **3.1 Quantification of missing VOC_R during the campaign**

204 **Figure 1** shows the time series of measured RO_H , calculated RO_H according to all
205 measured reactive gases, and missing VOC_R (the gap between measured and calculated
206 RO_H) in Guangzhou. By using PTR-ToF-MS, we measured many VOC species that
207 were difficult before. Besides the NMHCs species with carbons less than 12, PTR-ToF-
208 MS can also measure higher NMHCs with more carbons (C12–C20). With regard to
209 OVOCs, not only common OVOC species including formaldehyde and C2-C4
210 carbonyls but also some N-containing OVOC species such as nitrophenol, methyl
211 nitrophenol and several organic nitrates were measured. Thanks to these additional
212 measured VOCs, the measured RO_H was close to the calculated RO_H within 20% in most
213 periods. Nevertheless, there were still some days exhibiting remarkable missing VOC_R .
214 The days with missing VOC_R of more than 25% of total RO_H , namely high missing-
215 VOC_R days, are indicated by yellow background in **Fig. 1a**. The largest missing VOC_R
216 occurred on October 15th, 16th, 25th and 26th, with average values of 16 s^{-1} . During the
217 period of October 24th to 26th, the total RO_H was highest and the missing VOC_R was also
218 relatively high among all days. **Figure 1b** shows the contribution of different species
219 classifications to total RO_H during high missing- VOC_R days. Inorganic species,
220 NMHCs and OVOCs account for 34%, 13% and 14% of total RO_H , respectively, with
221 missing VOC_R accounting for 39%. The fraction of missing VOC_R (39%) during the
222 high missing- VOC_R days is comparable to measurements in Los Angeles 2010 (Griffith
223 et al., 2016) and in Seoul 2016 (Sanchez et al., 2021).

224 We evaluated the uncertainty of the missing VOC_R . The uncertainty of the RO_H
225 measurement was 15%. In addition, according to reports of Jet Propulsion Laboratory
226 (Burkholder et al., 2020), reaction rate constants used for the calculation of RO_H in Eq
227 (3) have uncertainties of 5%–30%, depending on different species. We took these
228 uncertainties into account when calculating RO_H , according to error propagation. As the



229 result, the uncertainties in the missing VOC_R are 3.8 s^{-1} and 5.2 s^{-1} for the whole
230 measurement period and the high missing- VOC_R days, respectively. The average
231 missing VOC_R during the high missing- VOC_R days is 12.3 s^{-1} , which is significantly
232 higher than the uncertainty of 5.2 s^{-1} , suggesting that the missing VOC_R really exists
233 during the high missing- VOC_R days.

234

235 **3.2 The sources of missing VOC_R**

236 To explore the sources of missing VOC_R during the whole measurement period,
237 we investigated the correlation between missing VOC_R and tracers characterizing
238 primary emissions (CO , NO_X and NMHCs) and secondary production ($\text{O}_X \equiv \text{O}_3 + \text{NO}_2$
239 and formic acid). The correlation of missing VOC_R with CO , reactivity of NMHCs
240 (NMHC_R) and NO_X is moderate, with correlation coefficient (R) in the range of 0.47–
241 0.56 (**Fig. 2a and b, and Fig. S1**) while there is no significant correlation of missing
242 VOC_R with O_X and formic acid (**Fig. 2c and Fig. S1**). Furthermore, there is no
243 significant correlation between missing VOC_R and acetonitrile which is a tracer of
244 biomass burning (de Gouw et al., 2003; Wang et al., 2007) (**Fig. S1**), indicating that
245 biomass burning was not a major contributor to missing VOC_R during this campaign.
246 In terms of the diurnal variation, the missing VOC_R was higher in the morning (7:00–
247 10:00) and evening (18:00–22:00.) when the anthropogenic emissions, especially
248 vehicle exhaust were intensive, and was lower in the afternoon when the
249 photochemistry was most active (**Fig. 2d**). The diurnal profile of missing VOC_R was
250 similar to those of CO , NO_X and NMHC_R . In contrast, the diurnal profiles of secondary
251 species including O_X , formic acid and acetic acid, which peaked in the afternoon,
252 evidently differ from the diurnal profile of missing VOC_R (**Fig. S2**). Further, we
253 investigated the influence of air mass aging on missing VOC_R . The ratio of ethylbenzene
254 to m,p-xylene was used to characterize the aging degree of air masses (De Gouw et al.,
255 2005; Yuan et al., 2013). A higher ratio of ethylbenzene to m,p-xylene corresponds to a
256 higher aging degree of air masses as the m,p-xylene has a larger reaction rate constant



257 than ethylbenzene when reacting with the major oxidant - OH radicals. As shown in
258 **Fig. 2e**, missing VOC_R decreases with the ratio of ethylbenzene to m,p-xylene. Given
259 that secondary production generally increased with air mass aging, this result further
260 demonstrates that missing VOC_R was not caused by enhanced secondary production.

261 Given the larger missing VOC_R level during the high missing- VOC_R days, we
262 focus on the high missing- VOC_R days in the following analysis. During the high
263 missing- VOC_R days, the correlation coefficient for missing VOC_R versus CO is 0.76
264 (**Fig. 3a**), which is higher than that in the whole measurement period (0.56) shown in
265 **Fig. 2a**. In addition, the correlation between missing VOC_R and O_X is weak with $R=$
266 0.25 during the high missing- VOC_R days (**Fig. 3b**). We then quantify the sources of
267 missing VOC_R during the high missing- VOC_R days by applying MLR. The coefficient
268 of determination (R^2) for the MLR is 0.68. As shown in **Fig. 3c**, anthropogenic
269 emissions were the largest contributor to missing VOC_R , accounting for 70% of missing
270 VOC_R . Secondary production, biogenic emissions and background contribution played
271 a minor role in missing VOC_R (13%, 7%, 10%, respectively). The parametric
272 relationship between missing VOC_R and relevant tracers established by MLR provides
273 a valid approach to estimate the missing VOC_R according to readily available gases
274 including CO, O_X and isoprene.

275 Although anthropogenic emissions are identified to be the major source of missing
276 VOC_R , which species dominantly contribute to the missing VOC_R remains unclear. A
277 potential source is the unmeasured branched alkenes for their high reactivity, previously
278 observed from vehicle exhaust (Nakashima et al., 2010) and gasoline evaporation
279 emissions (Wu et al., 2015). Another possible source is emitted OVOCs with a more
280 complex functional group that cannot be accurately measured. In addition, directly
281 emitted semi-volatile and intermediate volatility organic compounds are also possible
282 sources of missing VOC_R (Stewart et al., 2021).

283 **3.3 The impact of missing VOC_R on O_3 sensitivity regimes**

284 The reaction of OH with VOCs is key to the propagation and amplification of OH



285 radicals, thus determining the ozone production rate (Tonnesen and Dennis, 2000). The
286 box model was used to evaluate the impact of missing VOC_R on the O₃ production rate
287 during high missing–VOC_R days. In the base scenario, the box model was constrained
288 by all measured inorganic and organic gases but the missing VOC_R was not considered.
289 To consider the missing VOC_R in the box model, we increased all measured NMHC
290 species by a factor that can compensates for the missing VOC_R. In addition, we also try
291 adding a single VOC species to represent the missing VOC_R. Three typical VOC species
292 were added respectively, including n-pentane, ethylene and toluene. **Figure 4** shows the
293 simulated P(O₃) for the base scenario and the one considering missing VOC_R. The
294 daytime average P(O₃) under the scenario considering missing VOC_R is a factor of 1.5-
295 4.5 for the results under the base scenario. The difference in added species has a large
296 effect on P(O₃). Adding toluene causes a larger increase in P(O₃) than adding n-pentane
297 or ethene, as toluene has a stronger ability to amplify the production of radicals. The
298 uncertainty in missing VOC_R leads to 13-17% uncertainties in the threshold of NO_X for
299 scenarios considering missing VOC_R.

300 O₃ precursor sensitivity depends on the dominant loss pathways of RO_X radicals
301 (RO_X=OH+HO₂+RO₂). O₃ production is NO_X-limited if the self-reaction of peroxy
302 radicals (HO₂ and RO₂) dominates the RO_X sink, and VOC-limited if the reaction of
303 NO₂ with OH dominates (Kleinman et al., 1997; Kleinman et al., 2001). Accordingly,
304 the ratio of RO_X sink induced by OH+NO₂ reaction to the total rate of the two RO_X
305 sinks, i.e., L_N/Q, is used to identify O₃ sensitivity regimes. O₃ production is NO_X-
306 limited if L_N/Q is lower than 0.5, otherwise, it is VOC-limited (Kleinman et al., 1997).

$$307 \quad L_N/Q = \frac{k_{OH+NO_2}[OH][NO_2]}{k_{HO_2+RO_2}[HO_2][RO_2]+k_{HO_2+HO_2}[HO_2][HO_2]+k_{OH+HO_2}[OH][HO_2]+k_{OH+NO_2}[OH][NO_2]}$$

308 (7)

309 As shown in **Fig. 5a**, under the base scenario, L_N/Q remained at a stable and high
310 level (>0.9) during the daytime when photochemical production of ozone occurs,
311 indicating O₃ production was VOC-limited. Under the scenario considering missing
312 VOC_R, L_N/Q decreased significantly regardless of which VOC species was added,
313 compared to the base scenario. Adding toluene caused the largest decrease in L_N/Q,



314 followed by adding all measured NMHC species, adding the alkane and adding the
315 alkene. It is worth noting that adding toluene and all measured NMHC species caused
316 the L_N/Q to be close to 0.5 in the afternoon, indicating that the O_3 production shifted to
317 transitional or NO_X -limited regimes in these scenarios. **Fig. 5b** shows the changes in
318 radical sinks before and after considering missing VOC_R . All radical sinks including
319 self-reactions of peroxy radicals and $OH+NO_2$ reaction increased after considering
320 missing VOC_R . Nevertheless, the increased proportion of the self-reactions of peroxy
321 radicals was larger than that of $OH+NO_2$ reaction, leading to a decrease in L_N/Q and
322 thus a shift toward NO_X -limited regime.

323 **Figure 5c** shows the dependence of daily peak O_3 concentrations on NO_X
324 concentrations, which was calculated by the box model for the base scenario and the
325 scenario considering missing VOC_R . The NO_X concentration level corresponding to the
326 maximum of O_3 concentrations was determined. This NO_X concentration level reflects
327 the threshold to distinguish between VOC-limited and NO_X -limited regimes. The larger
328 threshold of NO_X represents a higher possibility of ozone production in NO_X limited
329 regime. The threshold of NO_X for the scenario considering missing VOC_R is 46% higher
330 than for the base scenario. Note that the uncertainty in missing VOC_R leads to 17%
331 uncertainty in the threshold of NO_X for the scenario considering missing VOC_R . Overall,
332 **Fig. 5** suggests that omitting the missing VOC_R will overestimate the degree of the
333 VOC-limited regime and thus overestimate the effect of VOCs abatement in reducing
334 ozone pollution, which in turn may mislead ozone control strategy.

335 **4 Conclusions**

336 Although many previous studies have reported that photochemical production
337 processes and biogenic emissions are important sources of missing VOC_R (Lou et al.,
338 2010;Dolgorouky et al., 2012;Yang et al., 2017;Sanchez et al., 2021;Di Carlo et al.,
339 2004), we find that anthropogenic emissions may dominate the missing VOC_R in urban
340 regions. In zero-dimensional box models and three-dimensional chemistry-transport
341 models, the input of VOCs emission information mainly contains well-studied simple-



342 structure alkanes, alkenes and aromatics, while those unmeasured/unknown VOC
343 species have been neglected. This will lead to biases in quantifying ozone production
344 and diagnosing ozone sensitivity regimes. Our study demonstrates that the ambient
345 measurement of R_{OH} at urban sites can provide quantification of missing VOC_R , which
346 can be used in models to account for the missing VOC_R from anthropogenic emissions.
347 In addition, the parametric equation of missing VOC_R versus CO developed here can
348 be used to estimate missing VOC_R according to CO measurements. Besides CO, other
349 specific classes of hydrocarbons are also expected to be used as tracers for the
350 development of the parametric equation. Further study should try to parse the specific
351 sources of the missing VOC_R , e.g., whether the missing VOC_R is from intermediate-
352 volatility and semi-volatile organic compounds emitted from vehicles or whether it is
353 from some other sources. Furthermore, future studies can focus on direct measurements
354 of missing VOC_R for various emission sources to develop a comprehensive emission
355 inventory of missing VOC_R , which will help to improve O_3 pollution mitigation
356 strategies.

357

358 **Acknowledgement**

359 This work was supported by the National Natural Science Foundation of China (grant
360 No. 42121004, 42275103, 42230701, 42175135). This work was also supported by
361 Special Fund Project for Science and Technology Innovation Strategy of Guangdong
362 Province (Grant No.2019B121205004).

363

364 **Competing interests**

365 Two of the authors (Dr. Hang Su and Dr. Yafang Cheng) are members of the editorial
366 board of ACP.

367

368 **References**

369 Atkinson, R.: Atmospheric chemistry of VOCs and NO_x , *Atmos. Environ.*, 34, 2063-2101, 2000.
370 Atkinson, R., and Arey, J.: Atmospheric degradation of volatile organic compounds, *Chemical*
371 *reviews*, 103, 4605-4638, 2003.



- 372 Burkholder, J., Sander, S., Abbatt, J., Barker, J., Cappa, C., Crounse, J., Dibble, T., Huie, R., Kolb,
373 C., and Kurylo, M.: Chemical kinetics and photochemical data for use in atmospheric studies;
374 evaluation number 19, Pasadena, CA: Jet Propulsion Laboratory, National Aeronautics and
375 Space ..., 2020.
- 376 De Gouw, J., Middlebrook, A., Warneke, C., Goldan, P., Kuster, W., Roberts, J., Fehsenfeld, F.,
377 Worsnop, D., Canagaratna, M., and Pszenny, A.: Budget of organic carbon in a polluted
378 atmosphere: Results from the New England Air Quality Study in 2002, *J. Geophys. Res.-*
379 *Atmos.*, 110, 2005.
- 380 de Gouw, J. A., Warneke, C., Parrish, D. D., Holloway, J. S., Trainer, M., and Fehsenfeld, F. C.:
381 Emission sources and ocean uptake of acetonitrile (CH₃CN) in the atmosphere, *J. Geophys.*
382 *Res.-Atmos.*, 108, <https://doi.org/10.1029/2002JD002897>, 2003.
- 383 Di Carlo, P., Brune, W. H., Martinez, M., Harder, H., Leshner, R., Ren, X. R., Thornberry, T., Carroll,
384 M. A., Young, V., Shepson, P. B., Riemer, D., Apel, E., and Campbell, C.: Missing OH
385 reactivity in a forest: Evidence for unknown reactive biogenic VOCs, *Science*, 304, 722-725,
386 10.1126/science.1094392, 2004.
- 387 Dolgorouky, C., Gros, V., Sarda-Estève, R., Sinha, V., Williams, J., Marchand, N., Sauvage, S.,
388 Poulain, L., Sciare, J., and Bonsang, B.: Total OH reactivity measurements in Paris during the
389 2010 MEGAPOLI winter campaign, *Atmos. Chem. Phys.*, 12, 9593-9612, 10.5194/acp-12-
390 9593-2012, 2012.
- 391 Fuchs, H., Tan, Z., Lu, K., Bohn, B., Broch, S., Brown, S. S., Dong, H., Gomm, S., Häsel, R., He,
392 L., Hofzumahaus, A., Holland, F., Li, X., Liu, Y., Lu, S., Min, K. E., Rohrer, F., Shao, M., Wang,
393 B., Wang, M., Wu, Y., Zeng, L., Zhang, Y., Wahner, A., and Zhang, Y.: OH reactivity at a rural
394 site (Wangdu) in the North China Plain: contributions from OH reactants and experimental OH
395 budget, *Atmos. Chem. Phys.*, 17, 645-661, 10.5194/acp-17-645-2017, 2017.
- 396 Goldstein, A. H., and Galbally, I. E.: Known and unexplored organic constituents in the earth's
397 atmosphere, *Environ. Sci. Technol.*, 41, 1514-1521, 2007.
- 398 Griffith, S. M., Hansen, R., Dusanter, S., Michoud, V., Gilman, J., Kuster, W., Veres, P., Graus, M.,
399 de Gouw, J., and Roberts, J.: Measurements of hydroxyl and hydroperoxy radicals during
400 CalNex-LA: Model comparisons and radical budgets, *J. Geophys. Res.-Atmos.*, 121, 4211-
401 4232, 2016.
- 402 Hansen, R. F., Griffith, S. M., Dusanter, S., Rickly, P. S., Stevens, P. S., Bertman, S. B., Carroll, M.
403 A., Erickson, M. H., Flynn, J. H., Grossberg, N., Jobson, B. T., Lefer, B. L., and Wallace, H.
404 W.: Measurements of total hydroxyl radical reactivity during CABINEX 2009 – Part 1:
405 field measurements, *Atmos. Chem. Phys.*, 14, 2923-2937, 10.5194/acp-14-2923-2014, 2014.
- 406 Hansen, R. F., Blocquet, M., Schoemaeker, C., Léonardis, T., Locoge, N., Fittschen, C., Hanoune,
407 B., Stevens, P. S., Sinha, V., and Dusanter, S.: Intercomparison of the comparative reactivity
408 method (CRM) and pump-probe technique for measuring total OH reactivity in an urban
409 environment, *Atmos. Meas. Tech.*, 8, 4243-4264, 10.5194/amt-8-4243-2015, 2015.
- 410 Jenkin, M. E., Saunders, S. M., Wagner, V., and Pilling, M. J.: Protocol for the development of the
411 Master Chemical Mechanism, MCM v3 (Part B): tropospheric degradation of aromatic volatile
412 organic compounds, *Atmos. Chem. Phys.*, 3, 181-193, 10.5194/acp-3-181-2003, 2003.
- 413 Kleinman, L. I.: Low and high NO_x tropospheric photochemistry, *J. Geophys. Res.-Atmos.*, 99,
414 16831-16838, 1994.
- 415 Kleinman, L. I., Daum, P. H., Lee, J. H., Lee, Y. N., Nunnermacker, L. J., Springston, S. R., Newman,



- 416 L., Weinstein-Lloyd, J., and Sillman, S.: Dependence of ozone production on NO and
417 hydrocarbons in the troposphere, *Geophys. Res. Lett.*, 24, 2299-2302, 1997.
- 418 Kleinman, L. I., Daum, P. H., Lee, Y. N., Nunnermacker, L. J., Springston, S. R., Weinstein-Lloyd,
419 J., and Rudolph, J.: Sensitivity of ozone production rate to ozone precursors, *Geophys. Res.
420 Lett.*, 28, 2903-2906, 2001.
- 421 Kovacs, T., Brune, W., Harder, H., Martinez, M., Simpasa, J., Frost, G., Williams, E., Jobson, T.,
422 Stroud, C., and Young, V.: Direct measurements of urban OH reactivity during Nashville SOS
423 in summer 1999, *Journal of Environmental Monitoring*, 5, 68-74, 2003.
- 424 Lefohn, A. S., Malley, C. S., Smith, L., Wells, B., Hazucha, M., Simon, H., Naik, V., Mills, G.,
425 Schultz, M. G., and Paoletti, E.: Tropospheric ozone assessment report: Global ozone metrics
426 for climate change, human health, and crop/ecosystem research, *Elem. Sci. Anth.*, 6, 2018.
- 427 Li, K., Jacob, D. J., Liao, H., Shen, L., Zhang, Q., and Bates, K. H.: Anthropogenic drivers of 2013–
428 2017 trends in summer surface ozone in China, *Proc. National Acad. Sci.*, 116, 422-427, 2019.
- 429 Li, X.-B., Yuan, B., Parrish, D. D., Chen, D., Song, Y., Yang, S., Liu, Z., and Shao, M.: Long-term
430 trend of ozone in southern China reveals future mitigation strategy for air pollution, *Atmos.
431 Environ.*, 269, 118869, 2022.
- 432 Lou, S., Holland, F., Rohrer, F., Lu, K., Bohn, B., Brauers, T., Chang, C., Fuchs, H., Häsel, R., and
433 Kita, K.: Atmospheric OH reactivities in the Pearl River Delta–China in summer 2006:
434 measurement and model results, *Atmos. Chem. Phys.*, 10, 11243-11260, 2010.
- 435 Lu, K. D., Hofzumahaus, A., Holland, F., Bohn, B., Brauers, T., Fuchs, H., Hu, M., Haseler, R., Kita,
436 K., Kondo, Y., Li, X., Lou, S. R., Oebel, A., Shao, M., Zeng, L. M., Wahner, A., Zhu, T., Zhang,
437 Y. H., and Rohrer, F.: Missing OH source in a suburban environment near Beijing: observed
438 and modelled OH and HO₂ concentrations in summer 2006, *Atmospheric Chemistry and
439 Physics*, 13, 1057-1080, 10.5194/acp-13-1057-2013, 2013.
- 440 Lu, X., Hong, J. Y., Zhang, L., Cooper, O. R., Schultz, M. G., Xu, X. B., Wang, T., Gao, M., Zhao,
441 Y. H., and Zhang, Y. H.: Severe Surface Ozone Pollution in China: A Global Perspective,
442 *Environ. Sci. Technol. Lett.*, 5, 487-494, 10.1021/acs.estlett.8b00366, 2018.
- 443 Mihelcic, D., Holland, F., Hofzumahaus, A., Hoppe, L., Konrad, S., Müsgen, P., Pätz, H. W., Schäfer,
444 H. J., Schmitz, T., and Volz-Thomas, A.: Peroxy radicals during BERLIOZ at Pabstthum:
445 Measurements, radical budgets and ozone production, *J. Geophys. Res.-Atmos.*, 108, 2003.
- 446 Monks, P. S., Archibald, A. T., Colette, A., Cooper, O., Coyle, M., Derwent, R., Fowler, D., Granier,
447 C., Law, K. S., Mills, G. E., Stevenson, D. S., Tarasova, O., Thouret, V., von Schneidmesser,
448 E., Sommariva, R., Wild, O., and Williams, M. L.: Tropospheric ozone and its precursors from
449 the urban to the global scale from air quality to short-lived climate forcer, *Atmos. Chem. Phys.*,
450 15, 8889-8973, 10.5194/acp-15-8889-2015, 2015.
- 451 Nakashima, Y., Kamei, N., Kobayashi, S., and Kajii, Y.: Total OH reactivity and VOC analyses for
452 gasoline vehicular exhaust with a chassis dynamometer, *Atmos. Environ.*, 44, 468-475,
453 <https://doi.org/10.1016/j.atmosenv.2009.11.006>, 2010.
- 454 Nakashima, Y., Kato, S., Greenberg, J., Harley, P., Karl, T., Turnipseed, A., Apel, E., Guenther, A.,
455 Smith, J., and Kajii, Y.: Total OH reactivity measurements in ambient air in a southern Rocky
456 mountain ponderosa pine forest during BEACHON-SRM08 summer campaign, *Atmos.
457 Environ.*, 85, 1-8, <https://doi.org/10.1016/j.atmosenv.2013.11.042>, 2014.
- 458 Nölscher, A. C., Yañez-Serrano, A. M., Wolff, S., de Araujo, A. C., Lavrič, J. V., Kesselmeier, J.,
459 and Williams, J.: Unexpected seasonality in quantity and composition of Amazon rainforest air



- 460 reactivity, *Nature Communications*, 7, 10383, 10.1038/ncomms10383, 2016.
- 461 Paoletti, E., De Marco, A., Beddows, D. C., Harrison, R. M., and Manning, W. J.: Ozone levels in
462 European and USA cities are increasing more than at rural sites, while peak values are
463 decreasing, *Environmental Pollution*, 192, 295-299, 2014.
- 464 Praplan, A. P., Tykka, T., Chen, D., Boy, M., Taipale, D., Vakkari, V., Zhou, P. T., Petaja, T., and
465 Hellen, H.: Long-term total OH reactivity measurements in a boreal forest, *Atmos. Chem.
466 Phys.*, 19, 14431-14453, 10.5194/acp-19-14431-2019, 2019.
- 467 Sadanaga, Y., Yoshino, A., Kato, S., and Kajii, Y.: Measurements of OH reactivity and
468 photochemical ozone production in the urban atmosphere, *Environ. Sci. Technol.*, 39, 8847-
469 8852, 2005.
- 470 Sanchez, D., Seco, R., Gu, D., Guenther, A., Mak, J., Lee, Y., Kim, D., Ahn, J., Blake, D., Herndon,
471 S., Jeong, D., Sullivan, J. T., McGee, T., Park, R., and Kim, S.: Contributions to OH reactivity
472 from unexplored volatile organic compounds measured by PTR-ToF-MS – a case study in a
473 suburban forest of the Seoul metropolitan area during the Korea–United States Air Quality
474 Study (KORUS-AQ) 2016, *Atmos. Chem. Phys.*, 21, 6331-6345, 10.5194/acp-21-6331-2021,
475 2021.
- 476 Sekimoto, K., Li, S.-M., Yuan, B., Koss, A., Coggon, M., Warneke, C., and de Gouw, J.: Calculation
477 of the sensitivity of proton-transfer-reaction mass spectrometry (PTR-MS) for organic trace
478 gases using molecular properties, *International Journal of Mass Spectrometry*, 421, 71-94,
479 10.1016/j.ijms.2017.04.006, 2017.
- 480 Shetter, R. E., and Müller, M.: Photolysis frequency measurements using actinic flux
481 spectroradiometry during the PEM-Tropics mission: Instrumentation description and some
482 results, *J. Geophys. Res.-Atmos.*, 104, 5647-5661, <https://doi.org/10.1029/98JD01381>, 1999.
- 483 Shirley, T. R., Brune, W. H., Ren, X., Mao, J., Leshner, R., Cardenas, B., Volkamer, R., Molina, L. T.,
484 Molina, M. J., Lamb, B., Velasco, E., Jobson, T., and Alexander, M.: Atmospheric oxidation in
485 the Mexico City Metropolitan Area (MCMA) during April 2003, *Atmos. Chem. Phys.*, 6, 2753-
486 2765, 10.5194/acp-6-2753-2006, 2006.
- 487 Sillman, S., Logan, J. A., and Wofsy, S. C.: The sensitivity of ozone to nitrogen oxides and
488 hydrocarbons in regional ozone episodes, *J. Geophys. Res.-Atmos.*, 95, 1837-1851, 1990.
- 489 Sinha, V., Williams, J., Crowley, J., and Lelieveld, J.: The Comparative Reactivity Method—a new
490 tool to measure total OH Reactivity in ambient air, *Atmos. Chem. Phys.*, 8, 2213-2227, 2008.
- 491 Stewart, G. J., Nelson, B. S., Acton, W. J. F., Vaughan, A. R., Farren, N. J., Hopkins, J. R., Ward, M.
492 W., Swift, S. J., Arya, R., Mondal, A., Jangirh, R., Ahlawat, S., Yadav, L., Sharma, S. K., Yunus,
493 S. S. M., Hewitt, C. N., Nemitz, E., Mullinger, N., Gadi, R., Sahu, L. K., Tripathi, N., Rickard,
494 A. R., Lee, J. D., Mandal, T. K., and Hamilton, J. F.: Emissions of intermediate-volatility and
495 semi-volatile organic compounds from domestic fuels used in Delhi, India, *Atmos. Chem.
496 Phys.*, 21, 2407-2426, 10.5194/acp-21-2407-2021, 2021.
- 497 Tonnesen, G. S., and Dennis, R. L.: Analysis of radical propagation efficiency to assess ozone
498 sensitivity to hydrocarbons and NO_x: 1. Local indicators of instantaneous odd oxygen
499 production sensitivity, *J. Geophys. Res.-Atmos.*, 105, 9213-9225, 2000.
- 500 Wang, C., Yuan, B., Wu, C., Wang, S., Qi, J., Wang, B., Wang, Z., Hu, W., Chen, W., Ye, C., Wang,
501 W., Sun, Y., Wang, C., Huang, S., Song, W., Wang, X., Yang, S., Zhang, S., Xu, W., Ma, N.,
502 Zhang, Z., Jiang, B., Su, H., Cheng, Y., Wang, X., and Shao, M.: Measurements of higher
503 alkanes using NO⁺ chemical ionization in PTR-ToF-MS: important contributions of higher



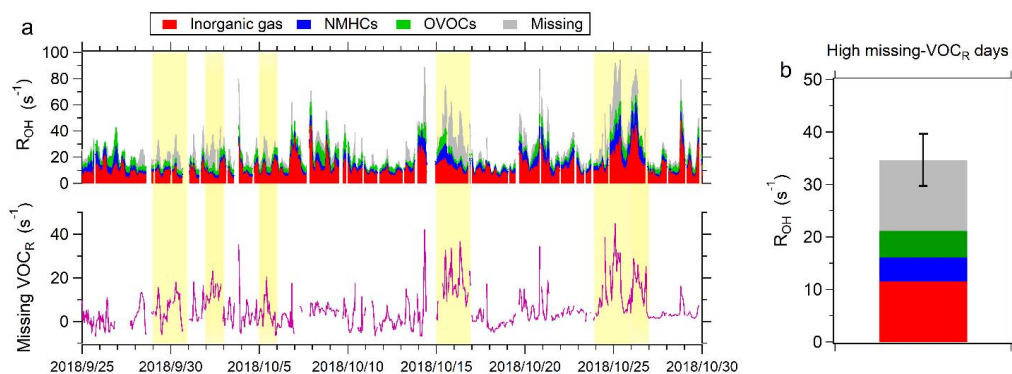
- 504 alkanes to secondary organic aerosols in China, *Atmospheric Chemistry and Physics*, 20,
505 14123-14138, 10.5194/acp-20-14123-2020, 2020a.
- 506 Wang, M., Zeng, L., Lu, S., Shao, M., Liu, X., Yu, X., Chen, W., Yuan, B., Zhang, Q., and Hu, M.:
507 Development and validation of a cryogen-free automatic gas chromatograph system (GC-
508 MS/FID) for online measurements of volatile organic compounds, *Anal. Methods*, 6, 9424-
509 9434, 2014.
- 510 Wang, Q. Q., Shao, M., Liu, Y., William, K., Paul, G., Li, X. H., Liu, Y. A., and Lu, S. H.: Impact
511 of biomass burning on urban air quality estimated by organic tracers: Guangzhou and Beijing
512 as cases, *Atmos. Environ.*, 41, 8380-8390, 10.1016/j.atmosenv.2007.06.048, 2007.
- 513 Wang, W., Li, X., Shao, M., Hu, M., Zeng, L., Wu, Y., and Tan, T.: The impact of aerosols on
514 photolysis frequencies and ozone production in Beijing during the 4-year period 2012–2015,
515 *Atmos. Chem. Phys.*, 19, 9413-9429, 10.5194/acp-19-9413-2019, 2019.
- 516 Wang, W., Parrish, D. D., Li, X., Shao, M., Liu, Y., Mo, Z., Lu, S., Hu, M., Fang, X., and Wu, Y.:
517 Exploring the drivers of the increased ozone production in Beijing in summertime during
518 2005–2016, *Atmos. Chem. Phys.*, 20, 15617-15633, 2020b.
- 519 Wang, W., Parrish, D. D., Wang, S., Bao, F., Ni, R., Li, X., Yang, S., Wang, H., Cheng, Y., and Su,
520 H.: Long-term trend of ozone pollution in China during 2014–2020: distinct seasonal and
521 spatial characteristics and ozone sensitivity, *Atmos. Chem. Phys.*, 22, 8935-8949, 10.5194/acp-
522 22-8935-2022, 2022.
- 523 Wu, C., Wang, C., Wang, S., Wang, W., Yuan, B., Qi, J., Wang, B., Wang, H., Wang, C., and Song,
524 W.: Measurement report: Important contributions of oxygenated compounds to emissions and
525 chemistry of volatile organic compounds in urban air, *Atmos. Chem. Phys.*, 20, 14769-14785,
526 2020.
- 527 Wu, Y., Yang, Y. D., Shao, M., and Lu, S. H.: Missing in total OH reactivity of VOCs from gasoline
528 evaporation, *Chinese Chemical Letters*, 26, 1246-1248, 10.1016/j.ccllet.2015.05.047, 2015.
- 529 Xie, X., Shao, M., Liu, Y., Lu, S., Chang, C.-C., and Chen, Z.-M.: Estimate of initial isoprene
530 contribution to ozone formation potential in Beijing, China, *Atmos. Environ.*, 42, 6000-6010,
531 2008.
- 532 Xu, R., Li, X., Dong, H., Lv, D., Kim, N., Yang, S., Wang, W., Chen, J., Shao, M., and Lu, S.: Field
533 observations and quantifications of atmospheric formaldehyde partitioning in gaseous and
534 particulate phases, *Sci. Total Environ.*, 808, 152122, 2022.
- 535 Yang, Y., Liao, H., and Lou, S.: Increase in winter haze over eastern China in recent decades: Roles
536 of variations in meteorological parameters and anthropogenic emissions, *J. Geophys. Res.-
537 Atmos.*, 121, 13,050-013,065, <https://doi.org/10.1002/2016JD025136>, 2016a.
- 538 Yang, Y., Shao, M., Wang, X., Nölscher, A. C., Kessel, S., Guenther, A., and Williams, J.: Towards
539 a quantitative understanding of total OH reactivity: A review, *Atmos. Environ.*, 134, 147-161,
540 2016b.
- 541 Yang, Y., Shao, M., Keßel, S., Li, Y., Lu, K., Lu, S., Williams, J., Zhang, Y., Zeng, L., Nölscher, A.
542 C., Wu, Y., Wang, X., and Zheng, J.: How the OH reactivity affects the ozone production
543 efficiency: case studies in Beijing and Heshan, China, *Atmos. Chem. Phys.*, 17, 7127-7142,
544 10.5194/acp-17-7127-2017, 2017.
- 545 Yoshino, A., Sadanaga, Y., Watanabe, K., Kato, S., Miyakawa, Y., Matsumoto, J., and Kajii, Y.:
546 Measurement of total OH reactivity by laser-induced pump and probe technique—
547 comprehensive observations in the urban atmosphere of Tokyo, *Atmos. Environ.*, 40, 7869-



- 548 7881, <https://doi.org/10.1016/j.atmosenv.2006.07.023>, 2006.
- 549 Yu, Y., Cheng, P., Li, H., Yang, W., Han, B., Song, W., Hu, W., Wang, X., Yuan, B., Shao, M., Huang,
550 Z., Li, Z., Zheng, J., Wang, H., and Yu, X.: Budget of nitrous acid (HONO) at an urban site in
551 the fall season of Guangzhou, China, *Atmos. Chem. Phys.*, 22, 8951-8971, 10.5194/acp-22-
552 8951-2022, 2022.
- 553 Yuan, B., Chen, W., Shao, M., Wang, M., Lu, S., Wang, B., Liu, Y., Chang, C.-C., and Wang, B.:
554 Measurements of ambient hydrocarbons and carbonyls in the Pearl River Delta (PRD), China,
555 *Atmos. Res.*, 116, 93-104, 2012.
- 556 Yuan, B., Hu, W., Shao, M., Wang, M., Chen, W., Lu, S., Zeng, L., and Hu, M.: VOC emissions,
557 evolutions and contributions to SOA formation at a receptor site in eastern China, *Atmos. Chem.*
558 *Phys.*, 13, 8815-8832, 2013.
- 559 Yuan, B., Koss, A. R., Warneke, C., Coggon, M., Sekimoto, K., and de Gouw, J. A.: Proton-Transfer-
560 Reaction Mass Spectrometry: Applications in Atmospheric Sciences, *Chemical Reviews*, 117,
561 13187-13229, 10.1021/acs.chemrev.7b00325, 2017.
- 562



563



564 **Figure 1. The level of missing VOC_R during the measurements in Guangzhou. (a)**

565 Time series of measured RO_H and calculated RO_H from all measured reactive gases in

566 Guangzhou. Yellow background represents the high missing- VOC_R days with missing

567 VOC_R accounting for more than 30% of total RO_H . (b) Contributions of different

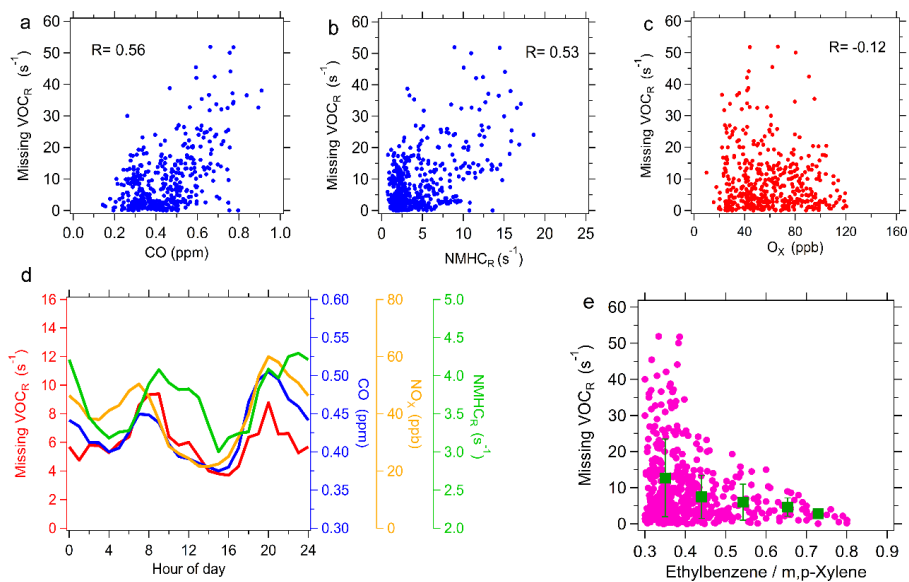
568 compositions to RO_H in high missing- VOC_R days. The error bar represents standard

569 deviation of missing VOC_R .

570

571

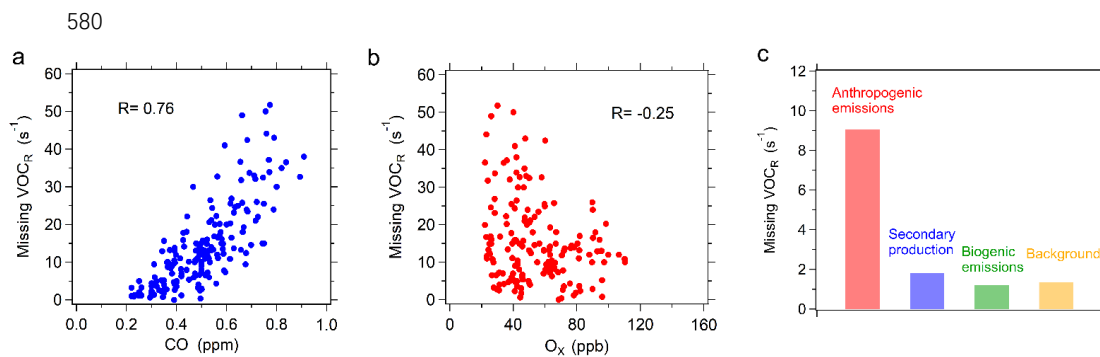
572



573

574 **Figure 2. Correlation of missing VOC_R with major tracers during the whole**
575 **measurement period. (a-c) Correlation of missing VOC_R with CO, OH reactivity of**
576 **NMHCs (NMHC_R) and O_X. Each point represents hourly data. (d) Diurnal variations**
577 **in missing VOC_R, CO, NO_X and NMHCs. (e) The dependence of missing VOC_R on**
578 **ethylbenzene to m, p-xylene ratio.**

579



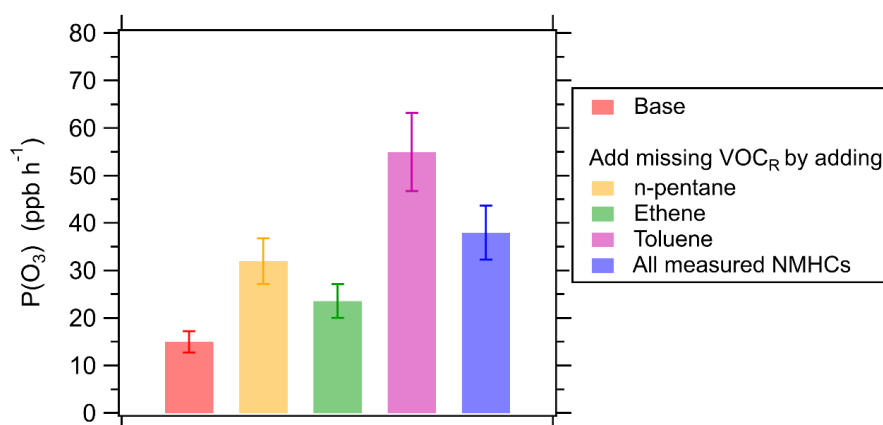


Figure 4. Simulated daytime mean $P(O_3)$ for the base scenario (without missing VOC_R) and the scenario considering missing VOC_R , respectively, in high-missing VOC_R days. The missing VOC_R is considered by adding individual species (n-pentane, ethene or toluene) or increasing all measured NMHCs to compensate for the missing VOC_R . The error bar represents standard deviation of $P(O_3)$ induced by the uncertainty of missing VOC_R .

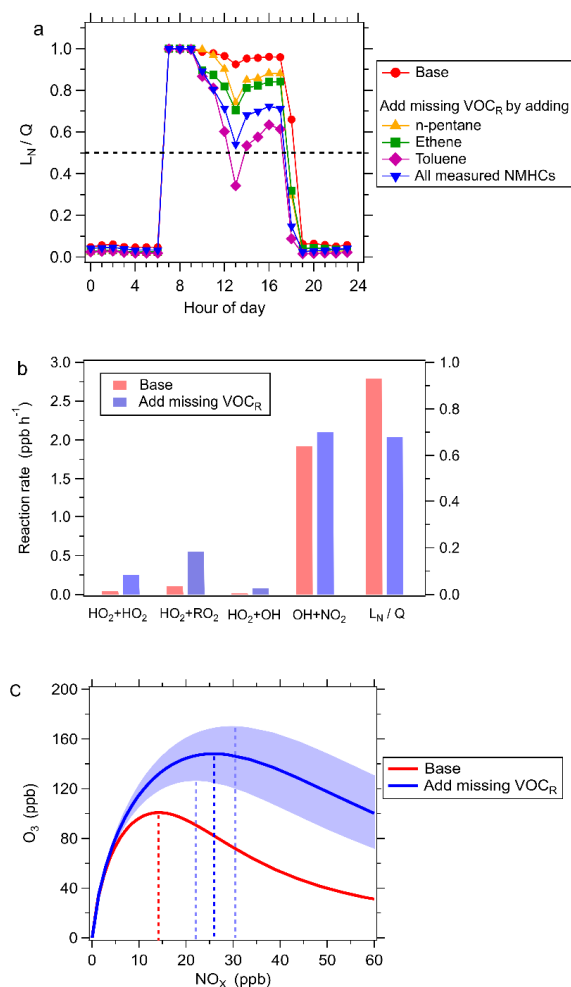


Figure 5. The impact of missing VOC_R on O₃ sensitivity for the high-missing VOC_R days. (a) Diurnal variations in L_N/Q for base scenario and the scenario considering missing VOC_R (blue bar). The missing VOC_R is considered by adding individual species (n-pentane, ethene or toluene) or increasing all measured NMHCs to fill the missing VOC_R. (b) The averages of radical sinks in the afternoon (12:00-18:00) for base scenario (red bar) and the scenario considering missing VOC_R (blue bar) by increasing all measured NMHCs to fill the missing VOC_R. (c) Model simulated dependence of daily peak O₃ concentrations on daily mean NO_x concentrations for base scenario (red curve) and the scenario considering missing VOC_R (blue curve) by increasing all



measured NMHCs to fill the missing VOC_R . The dashed lines parallel to Y-axis represent the threshold of NO_x levels to distinguish between VOC-limited and NO_x -limited regimes. The shaded area represents standard deviation induced by the uncertainty in missing VOC_R .